Original Article

Lip Vermilion Profile Patterns and Corresponding Dentoskeletal Forms in Female Adults

Chihiro Tanikawa[a]; Kayoko Nakamura[b]; Masakuzu Yagi[c]; Kenji Takada[d]

ABSTRACT

Objectives: To objectively classify shapes of the human lip vermilion in the lateral view, and to examine whether any morphologic characteristics of dentoskeletal patterns are specific to each classified lip profile pattern.

Materials and Methods: Pretreatment, lateral facial photographs of 234 Japanese women were selected. Investigators with expert knowledge of the anatomic traits of the lip vermilion in the lateral view extracted from images of the face a 13-dimensional feature vector that represented lip vermilion profile shapes. The vector quantization technique was applied to the feature vectors to mathematically optimize the number of lip vermilion profile patterns. Dentoskeletal patterns that corresponded to each classified lip shape were compared statistically.

Results: Seven patterns were found, and differences between patterns were notably maximized by the flatness of the anterior portion of the lip vermilion for the upper and lower lip, the position of the most protruded point of the lip vermilion, lip fissure inclination, and differences between the horizontal positions of the upper and lower lip vermilions. The dentoskeletal forms showed significant differences between classified lip vermilion profile patterns ($P < .01$).

Conclusions: (1) Vector quantization revealed that classifying lip vermilion profiles into seven representative patterns was optimal for maximizing differences in the configuration of the lip vermilion. (2) Lip vermilion profile shapes were found to be associated with horizontal lengths of the anterior cranial base, horizontal/vertical positions, inclination and length of the mandible, and horizontal positions and labio-lingual inclinations of the upper and lower incisors. (*Angle Orthod.* 2009;79:849–858.)

KEY WORDS: Lip vermilion; Profile; Classification

INTRODUCTION

The extent to which an individual's face is recognized by others exerts a great sociopsychological influence on that individual's sense of acceptance by his or her community. The lips are located in the lower third division of the face, and they play a key role in sustaining the quality of our life (ie, not only in terms of sustenance of biological life, but also in relation to proper pride as social beings).

When an orthodontic treatment plan is developed, evaluation of lip vermilion profile forms is indispensable in the decision of whether orthodontic movement of the incisors alone (camouflage) or a combined surgical orthodontic approach will more precisely create an improved posttreatment facial appearance. On the basis of these clinical demands, an objective and quantitative evaluation of morphologic traits of the lip vermilion in the lateral view would be of great value for making orthodontic diagnoses and for optimizing predictions of possible treatment outcomes. To date, several reports[1–6] have documented quantitative evaluations of the lip vermilion performed by means of linear and/or angular measurements with cephalograms (eg, distances between incisors and soft tissues, degrees of protrusion or retrusion). The results of these

[a] Assistant Professor, Department of Orthodontics and Dentofacial Orthopedics, Graduate School of Dentistry; Adjunct Assistant Professor, Center for Advanced Medical Engineering and Informatics, Osaka University, Suita, Japan.

[b] Former doctoral student, Department of Orthodontics and Dentofacial Orthopedics, Graduate School of Dentistry, Osaka University, Suita, Japan.

[c] Associate Professor, Center for Advanced Medical Engineering and Informatics, Osaka University, Suita, Japan.

[d] Professor and Chair, Department of Orthodontics and Dentofacial Orthopedics, Graduate School of Dentistry; Adjunct Professor, Center for Advanced Medical Engineering and Informatics, Osaka University, Suita, Japan.

Corresponding author: Dr Kenji Takada, Department of Orthodontics and Dentofacial Orthopedics, Graduate School of Dentistry, Osaka University, Suita, Osaka, Japan
(e-mail: opam@dent.osaka-u.ac.jp)

Accepted: December 2008. Submitted: October 2008.

reports are meaningful because the use of cephalograms allows simultaneous quantitative evaluation of hard and soft tissues; it is difficult, however, to identify lip commissures and lip vermilion borders from the cephalograms. A second problem is that the shape of the lip vermilion on cephalograms differed from that observed during visual inspection of the face (ie, the actual shape) because of a radial-tangential effect.[7] To resolve these issues, photographs were used in several reports to analyze the lip vermilion shape.[8–10] Because these analyses were conducted primarily with the use of linear and/or angular measurements, detailed morphologic characteristics of the entire lip vermilion (eg, pouty lip vermilion, flat lip vermilion, flaps of the lip vermilion) were not considered. Although Fourier series computations were found to be useful in obtaining and analyzing approximate entire human profiles,[11] they have not yet been applied to evaluation of the entire lip vermilion shape with a fine enough resolution to detect morphologic traits that, although they may be subtle, are significant in terms of an orthodontic diagnosis. Recently, a technique for modeling the feature extraction process that takes into account the knowledge and thought processes employed by experts in linguistically describing the morphologic traits of nose profiles has been established and confirmed to be of great value in orthodontic diagnoses.[12]

The purposes of the present study were (1) to determine the numbers and shapes of human lip vermilion profiles that are mathematically and thus objectively classifiable, and (2) to examine whether any unique morphologic characteristics of dentoskeletal patterns are specific to each classified soft tissue pattern.

MATERIALS AND METHODS

Two hundred thirty-four Japanese females who had never before received any orthodontic treatment were studied (mean age, 26 years 2 months; age range, 18 years 2 months to 59 years 1 month). These participants were selected consecutively from the patient database in order of their dates of registration at the hospital. The subjects had permanent dentition; none of them had any congenital anomalies, history of surgery, or trauma or injury to the face.

Conventional lateral facial photographs (right-side views) were employed. They were taken with the head fixed by ear rods and the Frankfort horizontal plane parallel to the ground, and with the upper and lower teeth in light intercuspation and the lips in repose. To examine the craniofacial morphologic characteristics of subjects, standard digitally recorded lateral cephalograms of each patient were used. Dentoskeletal traits of the subjects are summarized in Table 1. Proportions of subjects in terms of conventional sagittal skeletal classification[13] were as follows: skeletal Class I, 45.0%; skeletal Class II, 30.0%; and skeletal Class III, 25.0%.

Table 1. Summary of Subjects' Dentoskeletal Morphologic Traits[a]

Variable	Mean	SD	Minimum	Maximum	Normative Value[b]
SN, mm	69.2	3.1	59.0	80.4	67.9
SNA, degrees	81.5	3.5	70.6	96.9	80.8
A-Ptm/PP, mm	49.7	3.1	41.0	59.3	44.8
SNB, degrees	78.7	4.3	67.0	92.9	77.9
Ar-Me, mm	111.7	7.6	91.5	135.5	106.6
ANB, degrees	2.8	3.9	−8.2	12.0	2.8
SNMP, degrees	38.1	6.8	15.2	56.9	37.1
Me/PP, mm	72.3	7.5	49.0	132.0	68.6
U1-SN, degrees	106.4	8.4	73.6	134.7	105.9
L1-FH, degrees	57.2	10.2	29.7	93.0	56.0
OJ, mm	3.0	3.6	−7.7	11.0	3.2
OB, mm	2.0	2.7	−9.4	11.7	2.8

[a] SN indicates the distance between S and N; SNA, the SNA angle; A-Ptm/PP, A to Ptm distance projected on the palatal plane; SNB, the SNB angle; Ar-Me, the distance between Ar and Me; ANB, the ANB angle; SNMP, the angle formed by SN and the mandibular plane; Me/PP, the anterior lower face height; U1-SN, the angle formed by U1 and the SN plane; L1-FH, the angle formed by L1 and the FH plane; OJ, the overjet; and OB, the overbite.

[b] Female adults.[13]

The methods used for collection and analysis of data in the current study, including the definition of the coordinate system used in measuring the lateral face and the mathematical extraction of morphologic traits on the basis of human knowledge, have been described in detail elsewhere.[12] In this article, only a brief summary of the methods is provided.

An orthodontist visually located the positions of seven facial landmarks[9,12] (Table 2)—porion (po), exocanthion (ex), subnasale (sn), labiale superius (ls), labiale inferius (li), cheilion (ch), and stomion (sto)—on each photograph. The methods[12] used in segmenting the facial profile and in defining the coordinate system employed in the present study are schematically illustrated in Figure 1.

Twenty-eight descriptive parameters, expressed linguistically by t ($t = 1, 2, \ldots, 28$) and used in classifying the configuration of lip vermilions in the lateral view, were collected from a panel of three orthodontists, who provided their judgments based on experience and knowledge (Table 3).

On the basis of linguistic descriptions of the configurations of lip vermilions, 18 mathematical descriptions (ie, vector elements v1, v2, . . . , v18 and subsets of vector elements) were defined (Table 4, Figure 2).

Sixteen feature vector sets $V^{(w)}$ ($w = 1, 2, \ldots, 16$) that feature the configuration of the lip vermilion thus were determined with the use of vector elements (v1, v2, . . . , v18) or their combinations, with the conditions

Table 2. Definitions of the Landmarks Employed in the Present Study

Landmark	Definition
Porion (po)	The superior-most point of the ear rod
Exocanthion (ex)	The point at the outer commissure of the eye fissure
Subnasale (sn)	The point at which the columella merges with the upper cutaneous lip
Labiale superius (ls)	The point of intersection between the vermilion border of the upper lip and the cutaneous portion of the upper lip
Labiale inferius (li)	The point of intersection between the vermilion border of the lower lip and the cutaneous portion of the lower lip
Cheilion (ch)	The merged point of the upper and the lower vermilion arch
Stomion (sto)	The imaginary point at the crossing of the vertical facial midline and the horizontal labial fissure between gently closed lips, with teeth shut in the natural position
g	The geometric center of gravity of po, sn, and ex

previously reported.[12] Figure 3 shows the feature vector set that met these conditions. Shapes of the lip vermilion in the lateral view were classified, and the optimum vector set was identified.

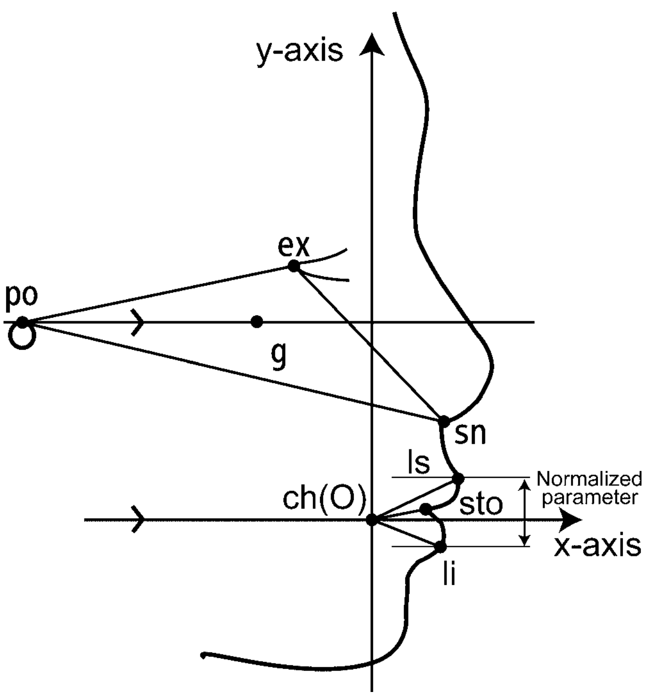

Figure 1. Schematic diagram illustrating the definition of the coordinate system. The ch was defined as the origin of the system. The *x*-axis was defined as a line parallel to the po-g line passing through the origin. The *y*-axis was defined as a line perpendicular to the *x*-axis through the origin. The position of the soft tissue landmarks and the contour data were defined mathematically and were normalized with respect to the difference in *y* coordinate values between ls and li.

Table 3. Twenty-eight Kinds of Knowledge Described in Linguistic Forms That Were Used for Classifying Shapes of Lip Vermilions

Linguistic Description	Parameter *t*
Form of the upper lip vermilion	
Thick	1
Thin	2
Round	3
Pointed	4
Flat	5
Vertical position of the most protruded point of the upper lip vermilion	
Upper	6
Lower	7
Form of the lower lip vermilion	
Thick	8
Thin	9
Round	10
Pointed	11
Flat	12
Vertical position of the most protruded point of the lower lip vermilion	
Upper	13
Lower	14
Relationship between the upper and lower lip vermilions	
Upper lip is more protruded	15
Lower lip is more protruded	16
Inclination of the lip fissure	
Upward	17
Downward	18
Length of the lip fissure	
Long	19
Short	20
Form of the entire lip vermilions	
Pouty lips	21
Full lips	22
Ripe lips	23
Thick lips	24
Thin lips	25
Everted lips	26
Flap-mouthed	27
Lips whose shapes seem to significantly change following anterior tooth retractions	28

A detailed description of methods used to calculate the optimum number of configurations of lip vermilion profile patterns (codes) and to identify an optimum feature vector set has been given.[12] In short, the vector quantization (VQ) method[14] was applied to feature vector sets to obtain the number of lip vermilion profile patterns that were mathematically optimized. Then, so that an optimum feature vector set could be identified out of $V^{(w)}$ ($w = 1, 2, \ldots, 16$), the matching score[12] for each feature vector set was calculated. The w that achieved the highest matching score was defined as the optimum feature vector extraction method.

Mean lip vermilion profile shapes reconstructed by averaging the approximated curves that connected ls and li and the linear curves that connected ch and ls,

Table 4. Definitions and Interpretations of 18 Vector Elements

Vector Element	Definition	Interpretation
v1	Distance between ch and ls	Length of the upper vermilion border
v2	Distance between ch and sto	Length of the lip fissure
v3	Distance between ch and li	Length of the lower vermilion border
v4	Distance between sto and ls	Thickness of the upper lip vermilion
v5	Distance between sto and li	Thickness of the lower lip vermilion
v6	L1/v4	Degree of flatness of the upper lip vermilion. Greater value means a more pointed upper lip vermilion
v7	L2/v4	Vertical position of the most protruded point of the upper lip vermilion
v8	L3/v5	Degree of flatness of the lower lip vermilion. Greater value means a more pointed lower lip vermilion
v9	L4/v5	Vertical position of the most protruded point of the lower lip vermilion
v10	Angle formed by ch-ls line and *x*-axis	Inclination of the upper lip vermilion border
v11	Angle formed by ch-li line and *x*-axis	Inclination of the lower lip vermilion border
v12	Angle formed by ch-sto line and *x*-axis	Inclination of the lip fissure. Greater value means a more upward lip fissure
v13	Difference in distance between ls and li on the *x*-axis	Sagittal upper and lower vermilion lip difference. A positive value is assigned if the ls is in a more forward position than the li
v14	Angle formed by ls-li line and *y*-axis	Sagittal upper and lower vermilion lip difference. A positive value is assigned if the ls is in a more forward position than the li
v15	Area surrounded by ls-sto line and ls-sto curve	Size of the anterior portion of the upper lip vermilion in the lateral view
v16	Area surrounded by li-sto line and li-sto curve	Size of the anterior portion of the lower lip vermilion in the lateral view
v17	L5/v4	Degree of flatness of the upper lip vermilion. Greater value means a flatter upper lip vermilion
v18	L6/v5	Degree of flatness of the lower lip vermilion. Greater value means a flatter lower lip vermilion

ch and sto, and ch and li, respectively for each code vector, were computed. Classified lip vermilion profile shapes were compared, as were the corresponding mean dentoskeletal patterns.

In examining the record sets that belonged to each extracted element of the feature vector, one-way analysis of variance (ANOVA) was performed to determine whether a significant difference could be seen between each element's code and each cephalometric variable as measured. In addition, the Tukey-Kramer test was performed to identify the codes that showed significant differences between the vector elements and between the cephalometric variables. A $P < .01$ level was assigned as significant.

RESULTS

The highest matching score was achieved when $w = 1$. In other words, the optimum feature vector was found to be a 13-dimensional vector whose elements were v1, v2, v3, v4, v5, v6, v7, v8, v9, v12, v13, v15, and v16. The shapes of lip vermilions in the current sample were found to be most effectively distinguished by the 13-dimensional feature vector thus determined in accordance with linguistic descriptions ($t = 1, 2, \ldots, 28$) that were assumed to reflect the knowledge and judgment shared by oral health practitioners who were experts on lateral lip shapes.

Seven mathematically optimized codes were identified. This means that the current samples typically exhibit seven types of lip vermilion profile shape. Proportions of the numbers of subjects classified into each code were, from Code 1 to Code 7, 23.5%, 18.4%, 15.8%, 15.4%, 14.5%, 9.8%, and 2.6%, respectively. Mean shapes of the lip vermilion profile patterns that corresponded to each of the seven codes are shown in Figure 4. Codes that were expressed in the real space are given in Table 5. Figure 5 reveals comparisons between codes for each vector element. A detailed description of differences in the shape of lip vermilions between codes is given in the Appendix.

Figure 6 shows comparisons of sample means and their standard deviations between the codes calculated for each cephalometric variable. Codes that were expressed in the real space are given in Table 6.

As for the length SN, Code 4 showed a significantly greater mean value when compared with Code 1 ($P < .01$). Regarding the maxilla, significant differences were not found between any codes for the angle SNA and the length A-Ptm/PP ($P < .01$). With regard to the mandible, Code 1, Code 3, Code 4, and Code 7 had significantly greater mean values than Code 5 for the length Ar-Me ($P < .01$). Code 5 had a significantly greater mean value than Code 6 for angle SNMP ($P < .01$). Code 1 had a significantly greater mean value

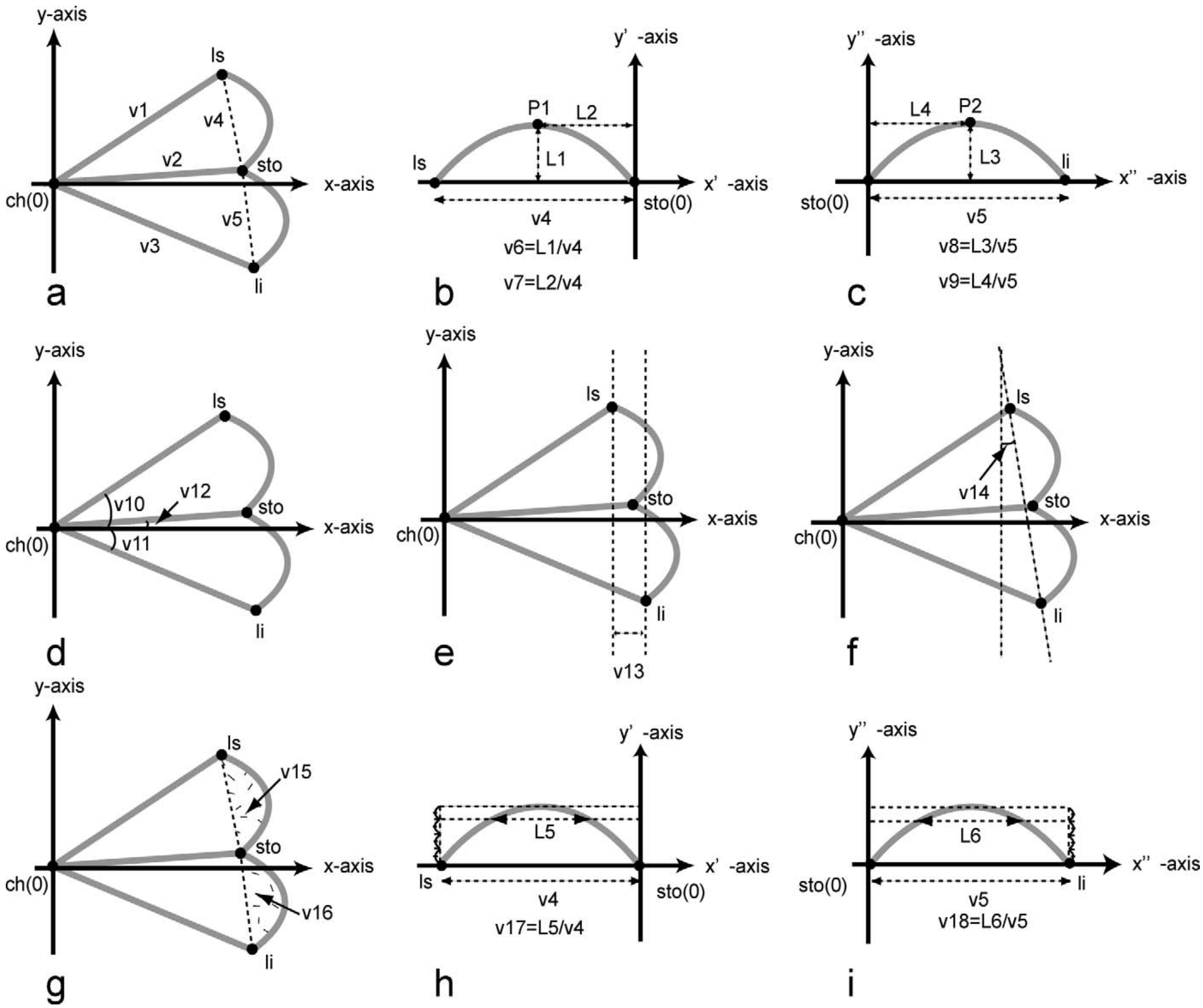

Figure 2. Schematic diagram illustrating the definitions of 18 vector elements employed in the present study. In a, d, e, f, and g, the ch was defined as the origin of the system: *x*-axis, a line parallel to the po-g line passing through the origin; *y*-axis, a line perpendicular to the *x*-axis through the origin; gray line, contour data of the lip vermilion; b and h, origin, sto; *x*′-axis, a line connecting sto and ls; *y*′-axis, a line perpendicular to the *x*′-axis that passes through the origin; gray line, contour data of the upper lip vermilion; P1, a point that showed the maximum *y*′ value of the upper lip contour; L1, *y*′ value of the P1; L2, *x*′ value of the P1; L5, distance between the intersections of the upper lip contour and a line parallel to the *x*′-axis at the 75% level of the peak height of the upper lip contour; c and i, origin, sto; *x*″-axis, a line that connects sto and li; *y*″-axis, a line perpendicular to the *x*″-axis through the origin; gray line, contour data of the lower lip vermilion; P2, a point that showed the maximum *y*″ value of the lower lip contour; L3, *y*″ value of the P2; L4, *x*″ value of the P2; and L6, distance between the intersections of the lower lip contour and a line parallel to the *x*″-axis at the 75% level of the peak height of the lower lip contour.

than Code 6 for the length Me/PP ($P < .01$). As for the angle ANB, Code 1, Code 3, Code 4, and Code 7 showed significantly smaller mean values than were seen in Code 5 ($P < .01$).

With regard to upper incisor inclination, Code 1 exhibited a significantly greater mean value than Code 5 for the angle U1-SN ($P < .01$). For the lower incisors, Code 2 and Code 5 represented significantly smaller mean values than Code 1 for the angle L1-FH ($P < .01$). Code 2, Code 5, and Code 6 showed significantly increased means compared with Code 1, Code 3, and Code 7 ($P < .01$). As for the overbite, Code 1 showed a significantly reduced mean value when compared with Code 2, Code 4, Code 5, and Code 6 ($P < .01$).

DISCUSSION

Relationships between dentoskeletal morphology and lip vermilion profile configuration have been documented most often on the basis of subjective obser-

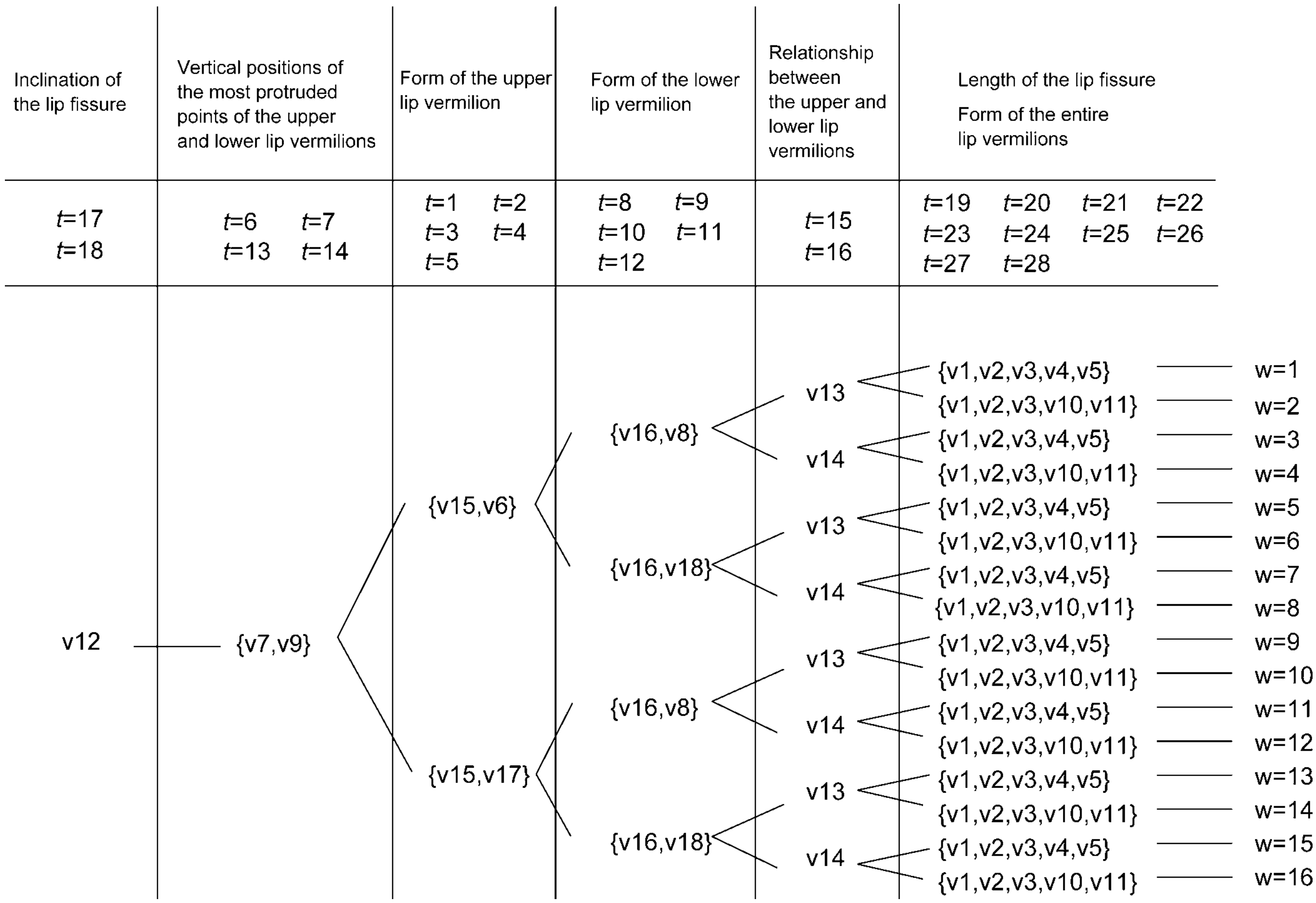

Figure 3. Tree diagram shows the combination of vector elements that constitute the feature vector representations $V^{(w)}$ (w = 1, 2, . . . , 16) and corresponding linguistic descriptions.

vation.[8] This is the first report that classified the human lip vermilion profile configuration objectively using the vector quantization method and determined its relationship to the underlying dentoskeletal morphology.

Code 2, Code 5, and Code 6 were characterized by forward posturing of the upper lip vermilion relative to the lower lip (see v13) and were associated with an increased overjet and a retruded mandible relative to the anterior cranial base. In other words, the results suggested that individuals with an increased overjet and the skeletal Class II tendency are likely to show more protrusive upper lip vermilions than lower lip vermilions. Code 2 was characterized by upper/lower lip vermilions whose anterior portions are large (often referred to as "protruded lips"; see v6, v8, v16). Code 6 represented the vertically long (often called a "thick or full lip"; see v4) upper lip vermilion whose anterior portion is large (see v6, v15) and the vertically shorter ("thin"; see v5) and flatter lower lip vermilion (see v16). Lip vermilion profile configurations of Code 2 and Code 6 were similar, but Code 6 exhibited a thicker and more protruded mean upper lip vermilion shape and a thinner lower lip vermilion shape, in contrast to Code 2. Such differences may be explained by the dentoskeletal morphologic traits as determined for Code 6 (ie, the tendency of lower incisors toward retroclination). It can be inferred that the tipped-in lower incisors as found in Code 6 subjects may likely lead to a backward positioning of the lower lip vermilion, forming a thinner appearance, whereas its upper counterpart may be looked upon as thicker (or vertically longer) because the upper lip vermilion receives, in theory, less vertical pressure from the lower lip vermilion. Code 5 was characterized by a lowered positioning of the most protruded point of the lower lip vermilion (see v9) and a straightforwardly oriented lip fissure (see v12). Mean dentoskeletal patterns characteristic of Code 5 included high mandibular angle tendency, palatally tipped upper incisors, and labially tipped lower incisors. It can be speculated that the lip vermilion in Code 5 is strained because the lip fissure tends to go upward in its posterior part when the subject must strain to bring the lips together. Code 5 is supposed to have inherent lip shortness in both upper

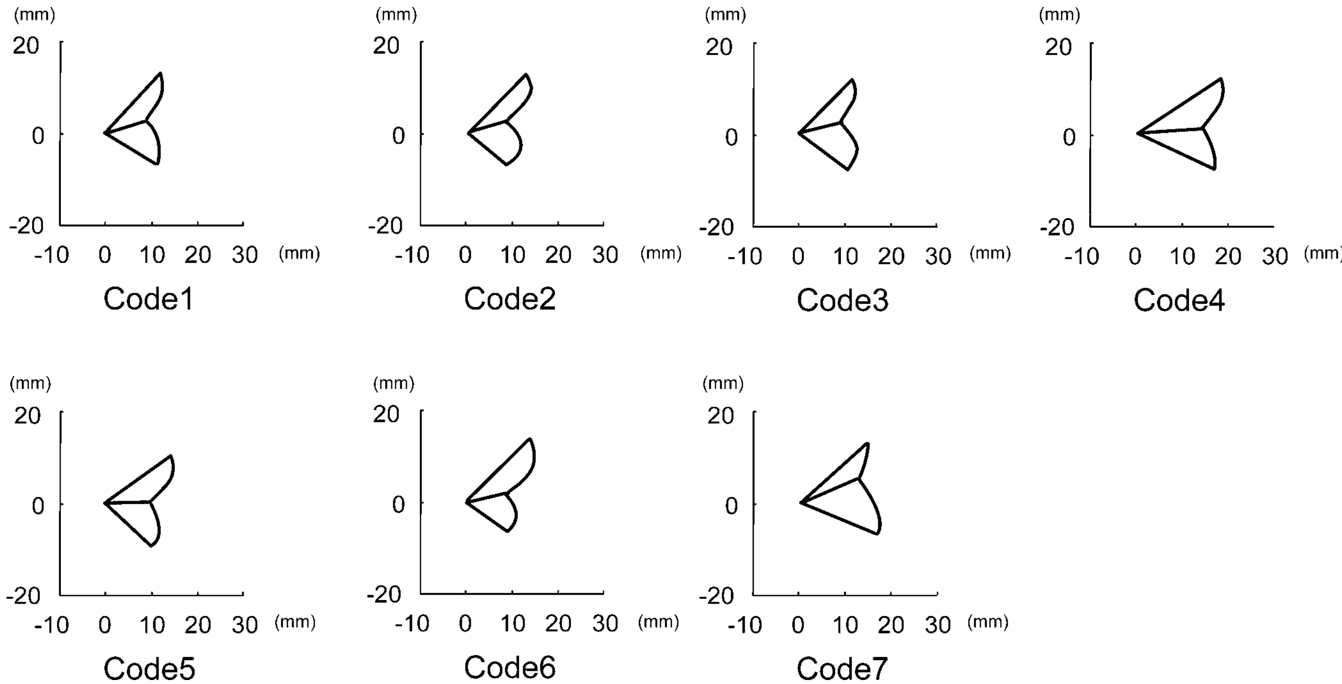

Figure 4. Mean configurations of the lip vermilion profiles that correspond to the seven codes. Origin indicates ch; *x*-axis, the line parallel to the line po-g that passes through the origin; and *y*-axis, the line perpendicular to the *x*-axis through the origin.

and lower lips because of the clockwise-rotated mandible, which leads to incongruity of lip structure with the skeletal pattern.[8]

Code 1, Code 3, and Code 7 exhibited a mean lip configuration that was characterized by a more forward position of the lower lip vermilion relative to the upper lip (see v13). Dentoskeletally, these are characterized by a decreased overjet and a skeletal Class III tendency accompanied by a longer mandibular effective length. It thus can be inferred that individuals who have a decreased incisor overjet and/or skeletal Class III morphologic traits are likely to show the more protruded lower lip vermilion when compared with the upper lip vermilion.

Both Code 3 and Code 7 had vertically shorter upper lip vermilions ("thin lip"; see v4) and longer lower lip vermilions ("chubby lip"; see v5). Two possible reasons can be put forth for such features. First, in individuals with skeletal mandibular prognathism, the lower lip vermilion, positioned more forward than its opponent, is likely to receive less vertically directed pressure from its upper counterpart (but rather greater pressure from the upper lip vermilion toward the forward direction), which results in the vertically thicker

Table 5. Means and Their Standard Deviations for Vector Elements Expressed in the Real Space Determined for Each Code[a,b]

	Code 1	Code 2	Code 3	Code 4	Code 5	Code 6	Code 7
v1	22.4 (2.2)	19.3 (2.5)	18.3 (2.3)	18.2 (1.7)	17.6 (1.8)	17.1 (2.4)	19.8 (5.4)
v2	15.3 (2.2)	9.4 (2.3)	9.6 (2.5)	10.7 (1.5)	9.6 (1.9)	9.8 (2.7)	14.5 (3.7)
v3	18.4 (2.7)	11.4 (1.9)	11.1 (1.9)	13.5 (1.5)	13.1 (2.1)	13.5 (1.8)	18.5 (5.3)
v4	11.1 (0.9)	12.0 (0.7)	10.5 (0.8)	10.6 (0.7)	10.7 (0.6)	9.6 (0.7)	9.1 (1.0)
v5	9.6 (0.9)	8.9 (0.5)	10.2 (0.6)	10.1 (0.6)	9.7 (0.6)	10.9 (0.6)	11.5 (1.5)
v6	0.2 (0.0)	0.2 (0.0)	0.2 (0.0)	0.2 (0.0)	0.2 (0.0)	0.1 (0.0)	0.0 (0.0)
v7	0.6 (0.1)	0.5 (0.1)	0.5 (0.0)	0.5 (0.0)	0.6 (0.0)	0.6 (0.1)	0.8 (0.0)
v8	0.1 (0.1)	0.2 (0.1)	0.3 (0.1)	0.2 (0.1)	0.2 (0.1)	0.2 (0.1)	0.2 (0.1)
v9	0.7 (0.1)	0.6 (0.1)	0.6 (0.0)	0.7 (0.0)	0.6 (0.1)	0.6 (0.0)	0.6 (0.1)
v12	7.0 (7.2)	16.7 (8.2)	20.0 (11.4)	5.3 (8.5)	17.3 (10.5)	17.6 (8.3)	15.3 (14.2)
v13	2.0 (3.2)	4.4 (2.8)	4.4 (2.6)	4.7 (2.2)	0.5 (2.2)	1.1 (3.0)	−2.0 (4.2)
v15	11.7 (4.2)	21.3 (4.5)	15.8 (4.4)	12.9 (3.0)	11.6 (2.9)	6.7 (2.5)	2.1 (2.1)
v16	5.8 (3.5)	10.2 (3.3)	21.3 (3.8)	10.3 (4.5)	9.9 (3.4)	17.6 (3.7)	12.6 (5.3)

[a] Unit, v1, v2, v3, v4, v5, v13: mm; v12: degree; v15, v16, mm^2.

[b] Note: Numbers in parentheses designate standard deviations.

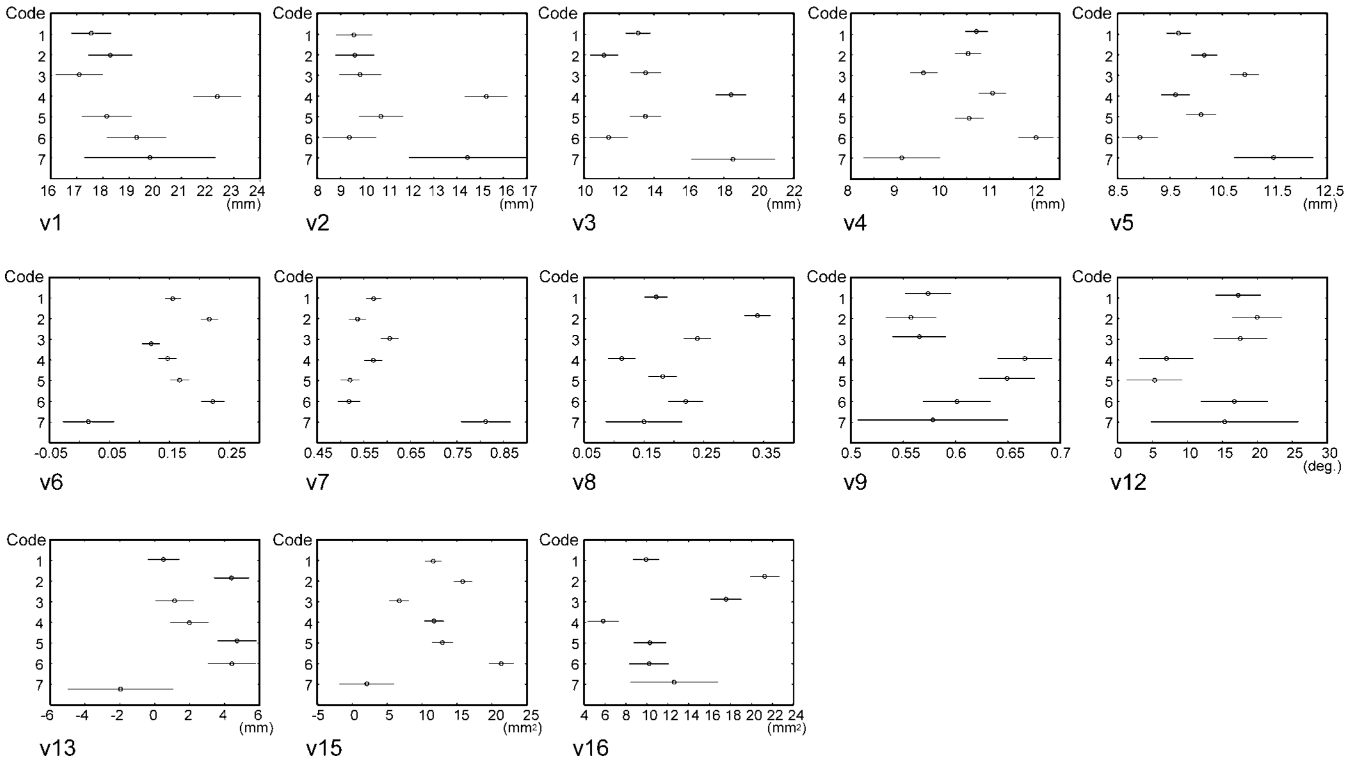

Figure 5. Intercode comparisons of sample means calculated for each of the 13 feature vector elements. *x*-axis indicates vector element values expressed in the real space; *y*-axis, code. Error bars represent Tukey-Kramer comparison intervals: nonoverlap between the bars of any two codes indicates that the hypothesis of no difference between the two was rejected at the $P < .01$ level. The circle points represent estimated means.

and horizontally protruded lower lip vermilion. In contrast, the upper lip vermilion acquires the vertically short (''thin'') and flat appearance. This may occur because the lower lip vermilion horizontally pushes the upper lip vermilion backward, and a part of the upper lip vermilion goes behind the lower lip vermilion. A second possibility is that Code 3 and Code 7 showed shortness in the upper lip, which leads to a thinner upper lip and thus a thicker lower lip as the result of less pressure from the upper lip vermilion. Code 1 does not exhibit the vertically shorter (i.e., thin) upper lip vermilion; this feature is unique to Code 1 among the lip configurations whose underlying hard tissue structures showed skeletal Class III tendencies. This

Table 6. Means and Their Standard Deviations Computed for Cephalometric Variables Determined for Each Code[a,b,c]

	Code 1	Code 2	Code 3	Code 4	Code 5	Code 6	Code 7
SN	70.7 (2.4)	69.7 (2.5)	69.6 (3.1)	69.3 (3.2)	68.4 (3.2)	68.6 (2.9)	69.2 (2.7)
SNA	81.5 (4.0)	81.6 (3.5)	81.6 (2.9)	81.2 (4.2)	81.8 (3.5)	81.4 (3.3)	80.3 (2.2)
A-Ptm/PP	50.0 (4.0)	49.5 (2.7)	50.3 (2.8)	49.7 (2.4)	49.6 (3.5)	48.9 (3.1)	49.5 (2.8)
SNB	79.3 (3.8)	78.0 (3.2)	76.8 (3.7)	75.0 (3.6)	80.5 (3.8)	80.2 (4.5)	81.8 (3.3)
Ar-Me	112.3 (5.8)	108.9 (4.4)	108.9 (7.2)	106.1 (6.1)	115.5 (8.0)	114.6 (6.5)	118.5 (7.5)
ANB	2.2 (3.7)	3.6 (2.7)	4.8 (3.4)	5.8 (3.0)	1.4 (3.8)	1.2 (3.6)	−1.5 (5.2)
SNMP	35.9 (6.2)	34.4 (5.4)	38.8 (7.1)	41.1 (7.3)	39.4 (6.9)	37.2 (5.5)	36.0 (5.7)
Me/PP	70.8 (6.3)	68.3 (5.4)	72.8 (11.9)	71.0 (4.6)	74.9 (6.8)	73.6 (5.2)	74.8 (6.0)
U1-SN	106.8 (8.6)	107.0 (11.0)	106.1 (8.3)	101.0 (7.9)	109.0 (6.8)	107.4 (8.0)	107.0 (6.6)
L1-FH	57.5 (9.6)	93.6 (9.1)	52.8 (8.4)	51.3 (10.4)	60.1 (9.8)	58.8 (10.7)	62.4 (8.9)
OJ	2.7 (3.1)	5.3 (2.7)	4.7 (2.9)	5.1 (2.5)	1.7 (3.3)	0.8 (3.9)	−1.5 (3.7)
OB	2.5 (2.0)	2.8 (3.2)	2.4 (2.8)	3.0 (1.8)	0.4 (2.9)	1.9 (2.5)	0.8 (2.2)

[a] SN indicates the distance between S and N; SNA, the SNA angle; A-Ptm/PP, A to Ptm distance projected on the palatal plane; SNB, the SNB angle; Ar-Me, the distance between Ar and Me; ANB, the ANB angle; SNMP, the angle formed by SN and the mandibular plane; Me/PP, the anterior lower face height; U1-SN, the angle formed by U1 and the SN plane; L1-FH, the angle formed by L1 and the FH plane; OJ, the overjet; and OB, the overbite.

[b] Unit, SN, A-Ptm/PP, Ar-Me, Me/PP, OJ, OB: mm; SNA, SNB, ANB, SNMP, U1-SN, L1-FH: degree.

[c] Note: Numbers in parentheses designate standard deviations.

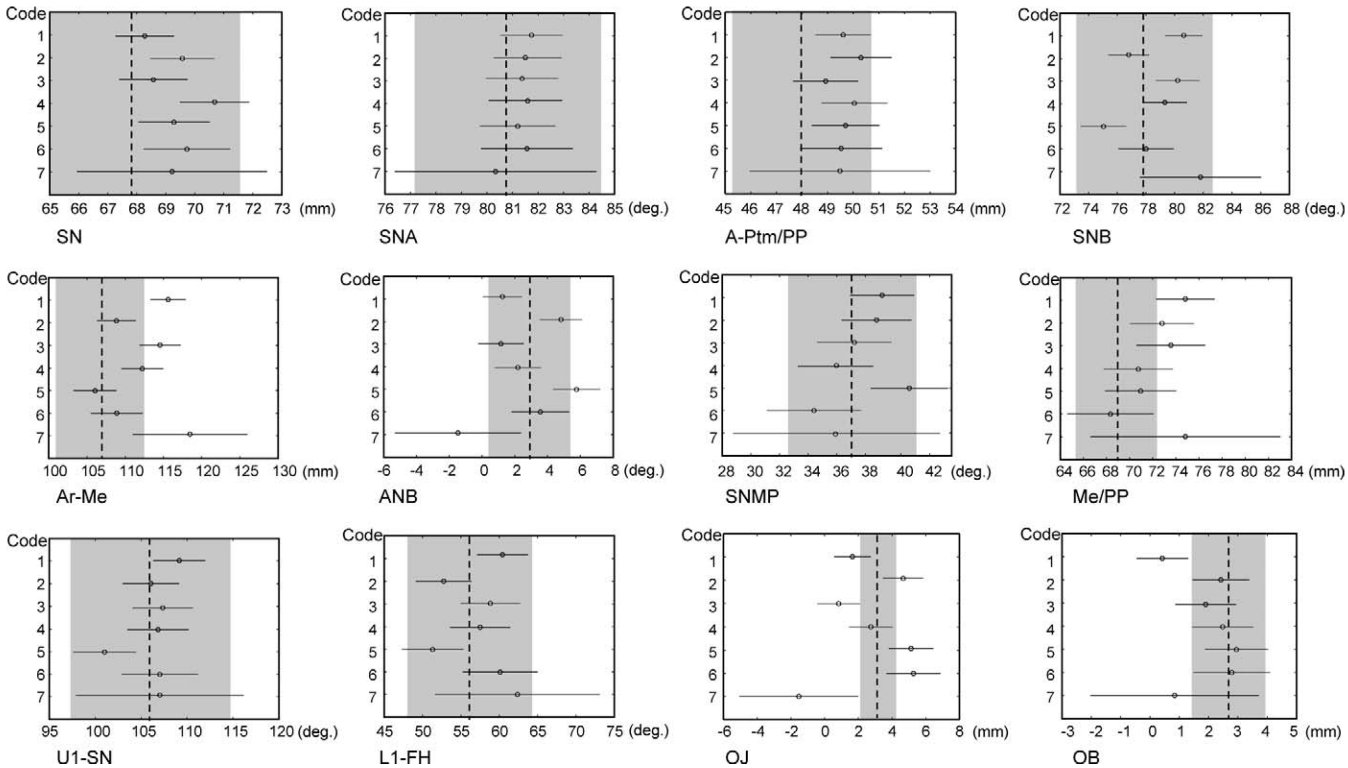

Figure 6. Intercode comparisons of the sample means calculated for each of the nine dentoskeletal variables. *x*-axis indicates measured values; *y*-axis, code. Dotted lines represent the means.[13] Shaded areas represent ranges encased by plus/minus one standard deviation[13] of the mean. Error bars represent Tukey-Kramer comparison intervals: nonoverlap between the bars of any two codes indicates that the hypothesis of no difference between the two was rejected at the $P < .01$ level. The circle points represent estimated means.

may be so because the severity of the mandibular prognathism in Code 1 was weaker than that in Code 3 or Code 7. In addition, subjects who constituted Code 1 showed labially inclined upper incisors. It can be speculated that the upper lip vermilion posture in Code 1 is dependent more on the underlying upper incisors than is the posture of those of other codes that showed skeletal Class III tendency; thus it pushes its lower counterpart vertically, which leads to the vertically even proportion of the upper and lower lip vermilions.

Code 4 was characterized by anteroposteriorly long lip vermilions (see v1, v2, v3), a flat lower lip vermilion (see v8, v9, v16), and the straightforwardly oriented fissure (see v12). As for the dentoskeletal features, the subjects who belong to Code 4 exhibited skeletal Class I relationships, a tendency toward the long mandibular effective length, and a long anterior cranial base, which translates to a horizontally large face. It can be speculated that, in a similar way as is found in Code 5, horizontal lip shortness in the upper and lower lips makes lips strained because of the incongruity of the lip structure with the horizontally large face; thus the lip fissure tends to go upward in its posterior part in strain, and the lip vermilion tends to be anteroposteriorly longer when the subject brings the lips together and purses the lips.[8]

In summary, lip vermilion profile configurations were found to be associated with horizontal lengths of the anterior cranial base, horizontal/vertical positions, inclination and length of the mandible, and horizontal positions and labio-lingual inclinations of the upper and lower incisors.

CONCLUSIONS

- The optimum knowledge description for distinguishing lip vermilion profile configurations was provided by a 13-dimensional feature vector representation.
- Classifying lip vermilion profile shapes collected from 234 women into seven representative patterns was optimum in maximizing differences in configuration of the lip vermilion.
- Proportions for each code (pattern) were 23.5%, 18.4%, 15.8%, 15.4%, 14.5%, 9.8%, and 2.6% from Code 1 to Code 7, respectively.
- Lip vermilion profile configurations were found to be associated with horizontal lengths of the anterior cranial base, horizontal/vertical positions, inclination and length of the mandible, and horizontal positions

and labio-lingual inclinations of the upper and lower incisors.

ACKNOWLEDGMENTS

This study was supported in part by the Global COE (Center of Excellence) Program "in silico medicine" at Osaka University and by a research grant from Shiseido Co, Ltd.

REFERENCES

1. Neger M, Newark NJ. A quantitative method for the evaluation of the soft-tissue facial profile. *Am J Orthod.* 1959;45:738–751.
2. Holdaway RA. A soft-tissue cephalometric analysis and its use in orthodontic treatment planning. Part I. *Am J Orthod.* 1983;84:1–28.
3. Lundström A, Forsberg CM, Peck S, McWilliam J. A proportional analysis of the soft tissue facial profile in young adults with normal occlusion. *Angle Orthod.* 1992;62:127–133.
4. Verdonck A, Jorissen E, Carels C, Van Thillo J. The interaction between soft tissues and the sagittal development of the dentition and the face. *Am J Orthod Dentofacial Orthop.* 1993;104:342–349.
5. Arnett GW, Jelic JS, Kim J, et al. Soft tissue cephalometric analysis: diagnosis and treatment planning of dentofacial deformity. *Am J Orthod Dentofacial Orthop.* 1999;116:239–253.
6. Bergman RT. Cephalometric soft tissue facial analysis. *Am J Orthod Dentofacial Orthop.* 1999;116:373–389.
7. Bjork A, Solow B. Measurement on radiographs. *J Dent Res.* 1962;41:672–683.
8. Ricketts RM. Esthetics, environment, and the law of lip relation. *Am J Orthod.* 1968;54:272–289.
9. Farkas L. *Anthropometry of the Head and Face.* 2nd ed. New York, NY: Raven Press Ltd; 1994.
10. Fernandez-Riveiro P, Smyth-Chamosa E, Suarez-Quintanilla D, Suarez-Cunqueiro M. Angular photogrammetric analysis of the soft tissue facial profile. *Eur J Orthod.* 2003;25:393–399.
11. Ferrario VF, Sforza C, Schmitz JH, Miani A Jr, Taroni G. Fourier analysis of human soft tissue facial shape: sex differences in normal adults. *J Anat.* 1995;187(Pt 3):593–602.
12. Tanikawa C, Kakiuchi Y, Yagi M, Miyata K, Takada K. Knowledge-dependent pattern classification of human nasal profiles. *Angle Orthod.* 2007;77:821–830.
13. Wada K. A study on the individual growth of maxillofacial skeleton by means of lateral cephalometric roentgenograms. *J Osaka Univ Dent Sch.* 1977;22:239–269.
14. Chang PC, Gray RM. Gradient algorithms for designing predictive vector quantizers. *IEEE Trans Acoust Speech Signal Process.* 1986;34:679–690.

APPENDIX

Detailed description of differences in shape of the lip vermilions between the codes

Code 4 designated a longer upper vermilion border than Code 1, Code 2, Code 3, Code 5 and Code 6 (See v1, $P < .01$). Code 7 represented longer lip fissures and longer lower vermilion borders than Code 1, Code 2, Code 3, Code 5 and Code 6 (See v2 and v3, $P < .01$).

Code 6 was designating the vertically longest upper lip vermilion and the vertically shortest lower lip vermilion (See v4 and v5, $P < .01$). On the other hand, Code 3 and Code 7 represented the vertically shortest upper lip vermilions and the vertically longest lower lip vermilions ($P < .01$).

Code 2 and Code 6 showed horizontally longer anterior portions of the upper lip vermilions (See v6, $P < .01$). Code 7 designated the sagittaly shortest anterior portion of the upper lip vermilion, and that the most protruded point of the upper lip vermilion was at the superior position (See v7, $P < .01$). Code 2 represented the horizontally longest anterior portion of the lower lip vermilion (See v8, $P < .01$). Code 4 and Code 5 designated that the most protruded points of the lower lip vermilions were at a lower position than Code 1, Code 2, and Code 3 (See v9, $P < .01$). Code 4 and Code 5 showed the lip fissures that went upward posteriorly (See v12, $P < .01$).

Code 2, Code 5, and Code 6 presented the relationships that the upper lip vermilion [ls] was in a more forward position than its opponent [li] (See v13, $P < .01$). Code 6 showed the largest anterior portion of the upper lip vermilion, and Code 3 and Code 7 demonstrated smaller anterior portions of the upper lip vermilions (See v15, $P < .01$). Code 2 showed the largest anterior portion of the lower lip vermilion and Code 4 showed the smallest anterior portion of the lower lip vermilion (See v16, $P < .01$).